Universiteit Leiden
The Netherlands

High-resolution magic angle spinning NMR studies for metabolic characterization of Arabidopsis thaliana mutants with enhanced growth characteristics

Augustijn, D.; Tol, N.V. van; Zaal, E.J. van der; Groot, H.J.M. de; Alia, A.

Citation
Augustijn, D., Tol, N. V. van, Zaal, E. J. van der, Groot, H. J. M. de, & Alia, A. (2018). High-resolution magic angle spinning NMR studies for metabolic characterization of Arabidopsis thaliana mutants with enhanced growth characteristics. *Plos One*, *13*(12), e0209695. doi:10.1371/journal.pone.0209695

Version: Publisher's Version
License: Creative Commons CC BY 4.0 license
Downloaded from: https://hdl.handle.net/1887/70284

Note: To cite this publication please use the final published version (if applicable).

PLOS ONE

RESEARCH ARTICLE

High-resolution magic angle spinning NMR studies for metabolic characterization of *Arabidopsis thaliana* mutants with enhanced growth characteristics

Dieuwertje Augustijn[1], Niels van Tol[2], Bert J. van der Zaal[2], Huub J. M. de Groot[1], A. Alia[1,3]*

1 Leiden Institute of Chemistry, Leiden University, RA Leiden, The Netherlands, **2** Institute of Biology Leiden, Leiden University, BE, Leiden, The Netherlands, **3** Institute of Medical Physics and Biophysics, University of Leipzig, Leipzig, Germany

* a.alia@chem.leidenuniv.nl

Check for updates

OPEN ACCESS

Citation: Augustijn D, Tol Nv, van der Zaal BJ, de Groot HJM, Alia A (2018) High-resolution magic angle spinning NMR studies for metabolic characterization of *Arabidopsis thaliana* mutants with enhanced growth characteristics. PLoS ONE 13(12): e0209695. https://doi.org/10.1371/journal.pone.0209695

Editor: Mohammed Bendahmane, Ecole Normale Superieure, FRANCE

Received: September 2, 2018

Accepted: December 10, 2018

Published: December 31, 2018

Copyright: © 2018 Augustijn et al. This is an open access article distributed under the terms of the Creative Commons Attribution License, which permits unrestricted use, distribution, and reproduction in any medium, provided the original author and source are credited.

Data Availability Statement: All relevant data are within the manuscript and its Supporting Information files.

Funding: This work was financially supported by the grant from Foundation for Fundamental Research on Matter, NL (http://www.fom.nl/live/english/home.pag) grant number FOM23 and by the grant from BioSolar Cell (http://www.biosolarcells.nl/) grant number U2.3. The funders had no role in study design, data collection and

Abstract

Developing smart crops which yield more biomass to meet the increasing demand for plant biomass has been an active area of research in last few decades. We investigated metabolic alterations in two *Arabidopsis thaliana* mutants with enhanced growth characteristics that were previously obtained from a collection of plant lines expressing artificial transcription factors. The metabolic profiles were obtained directly from intact *Arabidopsis* leaves using high-resolution magic angle spinning (HR-MAS) NMR. Multivariate analysis showed significant alteration of metabolite levels between the mutants and the wild-type Col-0. Interestingly, most of the metabolites that were reduced in the faster-growing mutants are generally involved in the defence against stress. These results suggest a growth-defence trade-off in the phenotypically engineered mutants. Our results further corroborate the idea that plant growth can be enhanced by suppressing defence pathways.

Introduction

During the last few decades, the demand for agricultural products has increased dramatically [1–3]. In order to meet the actual food demand in 2050, a 70% increase of the food production has to be realized in the coming three decades [4,5]. A possible way to meet this demand is to develop smart crops, varieties which can give more yield with fewer inputs [5,6]. This would also reduce the need for chemicals such as pesticides and fungicides.

New crop varieties with improved agronomic traits can be developed by traditional breeding methods [7], recently aided by the use of new genome-editing technologies such as provided by site-specific nucleases as CRISPR/CAS [8,9]. Recently, we have explored genome interrogation using zinc finger artificial transcription factors (ZF-ATFs) as a novel technique to drastically modify genome-wide transcription patterns and to generate novel phenotypes of interest in the model plant species *Arabidopsis thaliana* [9–12]. In these studies, arrays of three

analysis, decision to publish, or preparation of the manuscript.

Competing interests: The authors have declared that no competing interests exist.

zinc fingers (3F) were fused to the transcriptional activation domain of the VP16 protein of the herpes simplex virus [10]. Any 3F motif can recognize 9 base pairs of DNA, corresponding to approximately 1000 recognition sites in the nuclear *Arabidopsis* genome. Expression of a single 3F-VP16 fusion under control of the meristematic *RPS5A* promoter can thus lead to transcriptional activation of a large number of genomic loci, and consequently to drastic metabolic and phenotypic changes [9,11]. Previously, we have screened a population of transgenic Arabidopsis plants harbouring 3F-VP16 encoding gene constructs using enhanced rosette surface area (RSA) as a selection criterion for enhanced overall biomass accumulation [9,12]. From this phenotypic screen, we isolated two novel mutants designated VP16-02-003 and VP16-05-014 with respectively a 55% and 33% significantly larger RSA compared to the wild-type Col-0, each expressing a specific 3F-VP16 fusion protein. The growth differences did not relate to a differential development in the mutants as compared to the wild-type Col-0 [12]. In that previous study, a transcriptomics analysis was also performed to investigate the changes in the gene expression patterns [12]. Interestingly, we observed an overlap in the transcriptional changes in that correlated with the increase in RSA. Most notably, shared downregulated genes were found to be involved in several defence processes, including response to stress (GO:0006950), response to external stimulus (GO:0009605), response to wounding (GO:0009611), response to endogenous stimulus (GO:0009719), response to jasmonic acid (GO:0009753), response to stimulus (GO:0050896), defence response by cell wall thickening (GO:0052482) and defence response by callose deposition in cell wall (GO:0052544) (S1 Table) [12].

For a comprehensive understanding of newly developed plant genotypes, a systems biology approach is indispensable. Using this approach, a plant is seen as a system of interacting units that can be analysed as a whole rather than focusing on individual changes [6,13]. One of the system biology approaches is the metabolomics approach, which aims to determine small molecules that are involved in various physiological functions, such as growth, productivity and defence [14]. Directly examining the metabolic profiles of intact *Arabidopsis* leaves without any extraction is important to understand the functional framework of metabolism in the leaves. Recently, we have established high-resolution magic angle spinning nuclear magnetic resonance (HR-MAS NMR) to obtain the metabolic profile directly from intact wild-type *Arabidopsis* leaves [15].

In this study, we applied one- and two-dimensional HR-MAS NMR to obtain the metabolic profile directly from the intact leaves of wild-type Columbia (Col-0) *Arabidopsis* plants, and of the VP16-02-003 and VP16-05-014 mutants with enhanced growth characteristics and putatively higher sensitivity to biotic stress based on transcriptomics data. Through metabolic profiling in the native state in combination with multivariate analysis, we here provide novel insights into the biochemical pathways correlated to the enhanced rosette surface area phenotype for both mutants.

Materials & methods

Plant materials

Arabidopsis thaliana plants were grown in soil and cultivated in a growth chamber maintained at 293 K, 70% relative humidity and at a 12 h light (200 μmol m^{-2} s^{-1} photosynthetically active radiation) and 12 h dark regime [15]. Experiments were performed using the *Arabidopsis thaliana* accession Columbia-0 (Col-0) as wild-type. The VP16-02-003 and the VP16-05-014 mutant (both T3 generation) with an increased rosette surface area were obtained by phenotypic screening of a population of transgenic Arabidopsis plants harbouring 3F-VP16

encoding T-DNA constructs, as described previously [12]. The larger rosette surface area of both mutants are confirmed using ImageJ [12].

Quantification of free amino acids, soluble sugars, proteins and starch

The soluble sugar content was determined using the phenol-sulphuric acid method at a wavelength of 490 nm [16]. Glucose concentrations ranging from 0 to 250 μg/mL were used to obtain a standard curve. The free amino acids content was determined using the ninhydrin method as described previously [17]. Proteins were extracted from the leaves as described before [18]. Protein content was quantified by a Bradford assay [19]. The starch content of the leaves was measured by determining the glucose released with α-amylase and amyloglucosidase as described by Smith and Zeeman [20].

Statistical analysis

The data for each independent experiment were subjected to the Student's t-test. The OriginPro 2016 software (Northampton, USA) was used to determine the differences between Col-0 and the VP16-02-003 and VP16-05-014 mutants. Values are presented as means ± standard error (SEM) and statistical significance was determined at $p < 0.05$.

HR-MAS NMR-based metabolic profiling

The leaves were harvested from the plants at 28 days after germination (dpg, growth stage 3.70–3.90), frozen immediately in liquid nitrogen and stored at -80˚C until use. A single rosette leaf (0.0684 ± 0.0087 mg, 8 different plants for every genotype) was inserted into a 4 mm zirconium oxide (ZrO_2) rotor. 10 μl of deuterated phosphate buffer (100 mM, pH 6) containing 0.1% (w/v) 3-trimetylsilyl-2,2,3,3-tetradeuteropropionic acid (TSP) was added as a lock solvent and NMR reference. ^{1}H High-Resolution Magic Angle Spinning (HR-MAS) NMR experiments were performed with a Bruker DMX 400 MHz spectrometer operating at a resonance frequency of 399.427 MHz. The instrument is equipped with a 4 mm HR-MAS dual inverse ^{1}H/^{13}C probe with a magic angle gradient. Data were collected with a spinning frequency of 4 kHz at a temperature of 277 K.

The one-dimensional ^{1}H HR-MAS NMR spectra were recorded using a rotor synchronized Carr-Purcell-Meiboom-Gill (CPMG) pulse sequence with water suppression [21]. Each one-dimensional spectrum was acquired applying 256 transients, a spectral width of 8000 Hz, a data size of 16 K points, an acquisition time of 2 seconds and a relaxation delay of 2 seconds. The free induction decays (FIDs) were exponentially weighted with a line broadening of 1 Hz. Spectra were phased manually and automatically baseline corrected using TOPSPIN 2.1 (Bruker Analytische Messtechnik, Germany). A gradient-enhanced two-dimensional ^{1}H-^{1}H-COSY sequence was applied in order to confirm signal assignments as described before [14].

Multivariate analysis

A bucket table was generated from the one-dimensional spectra using AMIX software (version 3.8.7, BrukerBioSpin). The region between 4.20–6.00 ppm was excluded from the analysis to remove the large water signal. The one-dimensional CPMG spectra were normalized to the total intensity and binned into buckets of 0.04 ppm. The data was mean centred and the Pareto scaling method was used [22]. Unsupervised Principal Component Analysis (PCA) and supervised Orthogonal Projections to Latent Structures Discriminant Analysis (OPLS-DA) were performed on the bucket table using the SIMCA software package version 14.0 (Umetrics, Umeå, Sweden). The quality of these models was evaluated by the R^2X and R^2Y, the goodness-

of-fit parameters, and Q^2, a measure of the quality of the model based on cross-validation [23,24]. One sample from the VP16-05-014 dataset was removed as it was a significant outlier defined as an observation located outside the 95% confidence region of the Hotelling's T2 ellipse in the PCA scatter plot (see Supplementary S1 Fig) [25]. Further analysis was performed without this outlier. OPLS-DA was used to determine the buckets which are different between the mutants and the wild-type Col-0. In addition, two OPLS-DA models were constructed for each mutant; Col-0 vs VP16-02-003 and Col-0 vs VP16-05-014 (S2 Fig). The shared and unique structures between these two OPLS-DA models were investigated using a SUS (shared and unique structures) plot [26].

Biomarker identification

The metabolites corresponding to the peaks of interest in the determined buckets were identified by the Biological Magnetic Resonance Data Bank (BMRB) (www.bmrb.wisc.edu/metabolomics), Platform for RIKEN Metabolomics [27,28] and Chenomx NMR Suite 8.2 (Chenomx Inc., Edmonton, Alberta, Canada).

Quantification of metabolites

Chenomx NMR Suite 8.2 (Chenomx Inc., Edmonton, Alberta, Canada) was used for quantitative NMR data analysis. The concentrations of the various metabolites in the spectra of the leaves from wild-type and mutant *Arabidopsis* were determined by the known concentration of the reference peak of TSP. All Student's t-test analyses of the NMR quantification results were performed with OriginPro 2016 (Northampton, USA), The t-test is used after multivariate analysis (where correlation between metabolites was already taken into account).

Results and discussion

The larger rosette surface area phenotype of the VP16-02-003 and VP16-05-014 mutant was confirmed by determining the rosette surface area (RSA) at 28 days post germination (Fig 1). The VP16-02-003 and the VP16-05-014 mutant have respectively 53% and 31% larger RSA in comparison to Col-0. This is in line with our earlier publication on these *Arabidopsis* mutants [12].

Levels of free amino acids, soluble sugars, proteins and starch

Prior to metabolic profiling, the concentration of free amino acids, proteins, soluble sugars and starch was determined for extracts of leaves from the VP16-02-003 and VP16-05-014 mutant and Col-0 to get a broader overview of amino acids, sugars, protein and starch. Interestingly, an overall decline in free amino acids, soluble sugars, proteins, as well as starch content, was observed for the VP16-02-003 and VP16-05-014 mutants of *Arabidopsis* as compared to Col-0 (Table 1).

Sulpice *et al*. observed a negative correlation between biomass and the levels of starch, total protein and total free amino acids in *Arabidopsis* [29]. The level of soluble sugars such as sucrose has also found to be negatively correlated with biomass [29]. Sugars, such as glucose and sucrose are important products of photosynthesis and play an essential role in controlling plant growth, development and defence [14]. The decline in the level of soluble sugars accompanied by an increase in overall biomass and no significant difference in development of the two mutants indicates that sugar resources are likely diverted toward growth and storage products in these mutants, rather than defence-related processes.

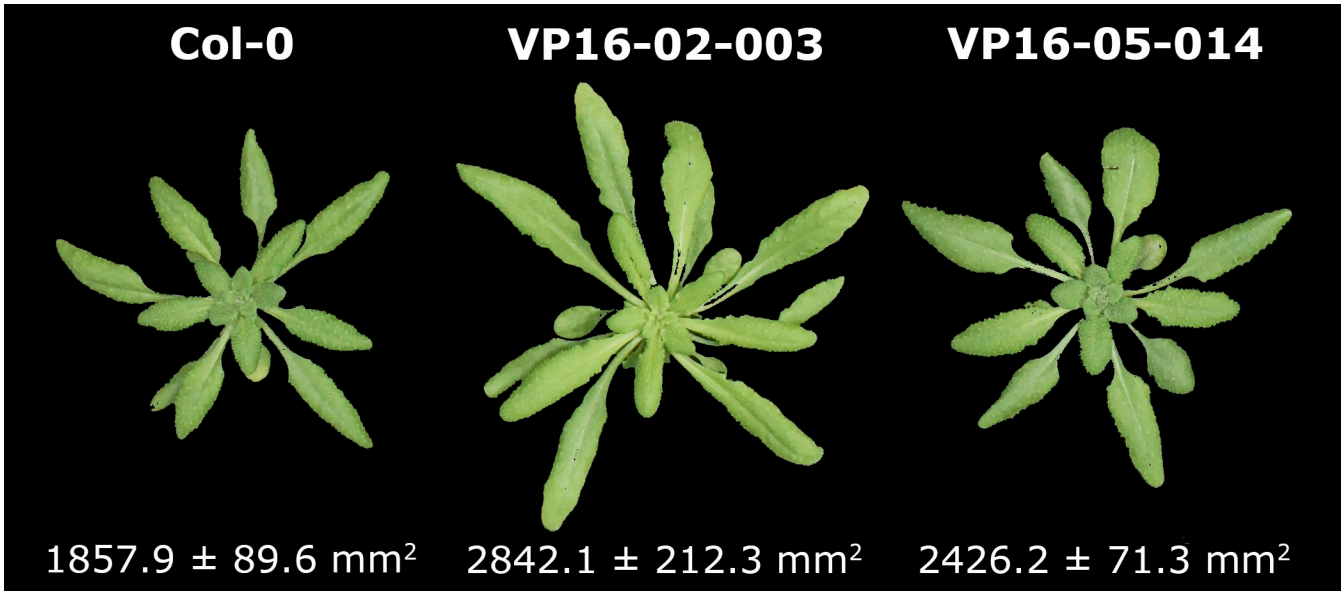

Fig 1. Representative overview of the rosette phenotypes of Arabidopsis Col-0, VP16-02-003 and VP16-05-014 at 28 days post germination. Data of average rosette surface area is shown below each images as mean ± SEM (n = 18).

https://doi.org/10.1371/journal.pone.0209695.g001

Metabolic profiling of the VP16-02-003 and VP16-05-014 mutant

In order to identify metabolites and biochemical pathways responsible for the increased rosette surface area shared phenotype of the VP16-02-003 and VP16-05-014 mutant, their metabolic profiles have been analysed for intact leaves using HR-MAS NMR. In Fig 2, representative one-dimensional ^{1}H NMR spectra of Col-0, VP16-02-003 and VP16-05-014 are shown. Two-dimensional homonuclear correlation spectroscopy (^{1}H-^{1}H COSY) enabled confirmation of metabolites by their spin systems. In addition, the 2D ^{1}H-^{1}H COSY data can be used to validate changes observed in the 1D spectral envelope for the mutants as compared to Col-0. The signals of various metabolites were assigned with the help of literature data from the Biological Magnetic Resonance Data Bank (BMRB) [30,31]. S2 Table shows a list of identified metabolites.

Identification of the increased rosette surface area shared phenotype

To probe if *Arabidopsis thaliana* Col-0, VP16-02-003 and VP16-05-014 can be discriminated from each other based on their metabolic profiles, multivariate analysis was applied to the HR-MAS spectra from both mutants and Col-0. Unsupervised PCA was performed which

Table 1. Total free amino acids, protein, soluble sugar and starch content in mg/g fresh weight for leaves of *Arabidopsis thaliana* Col-0, VP16-02-003 and VP16-05-014.

Content (mg/g FW)	Col-0	VP16-02-003	VP16-05-014
Free amino acids	1.48 ± 0.05	1.17 ± 0.05 *	1.04 ± 0.01 *
Protein	1.57 ± 0.06	1.34 ± 0.08 *	0.98 ± 0.01 *
Soluble sugar	0.18 ± 0.01	0.11 ± 0.01 *	0.13 ± 0.01 *
Starch	0.57 ± 0.02	0.23 ± 0.01 *	0.31 ± 0.02 *

Data is expressed as mean ± SEM (n = 5).

* $p < 0.05$ compared with Col-0

https://doi.org/10.1371/journal.pone.0209695.t001

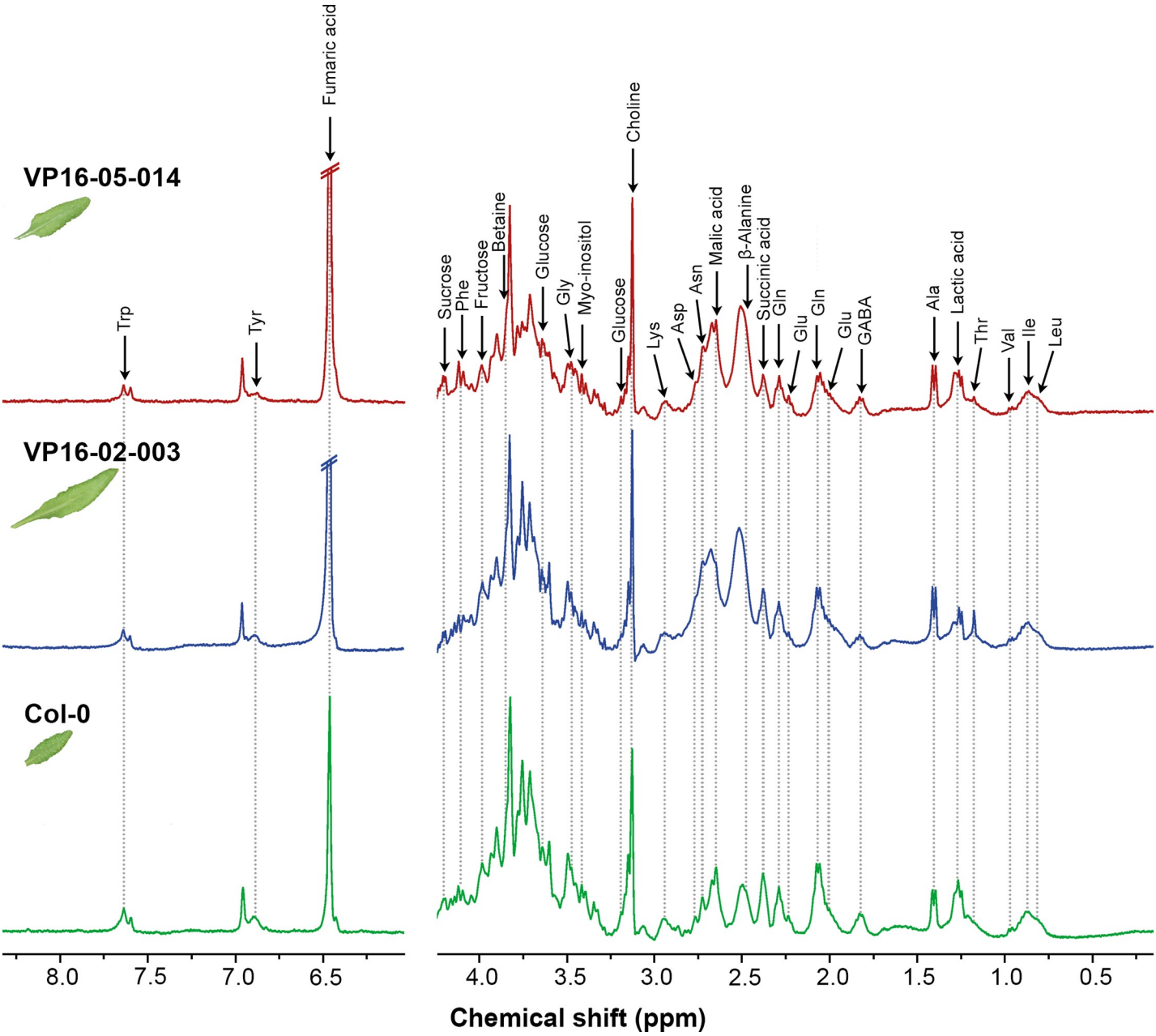

Fig 2. Representative one-dimensional ^{1}H HR-MAS NMR spectra collected from intact leaves of *Arabidopsis thaliana* Col-0 (bottom panels), VP16-02-003 (middle panels) and VP16-05-014 (top panels) grown in a 12h-light/12h-dark regime. The intact leaves were harvested 28 dpg at t = 6 hours (6 hours after the beginning of the light period) for the measurement. The signals from the assigned metabolites have been shown in the spectra (see S2 Table for assignment).

https://doi.org/10.1371/journal.pone.0209695.g002

explained 76.1% of the variation by a three-component model (see Fig 3A), which shows a clear group separation of VP16-05-014 from the Col-0 and VP16-02-003. In contrast, there was no clear group separation between Col-0 and VP16-02-003 in the PCA score plot. Supervised OPLS-DA was applied to further understand the separation between the wild-type Col-0, VP16-02-003 and VP16-05-014 and to identify crucial candidates biomarkers involved in the increased rosette surface area phenotype. Fig 3B shows the score plot of the OPLS-DA. The R^2X, R^2Y and Q^2 were 0.849, 0.942 and 0.603, respectively. The OPLS-DA model was found to

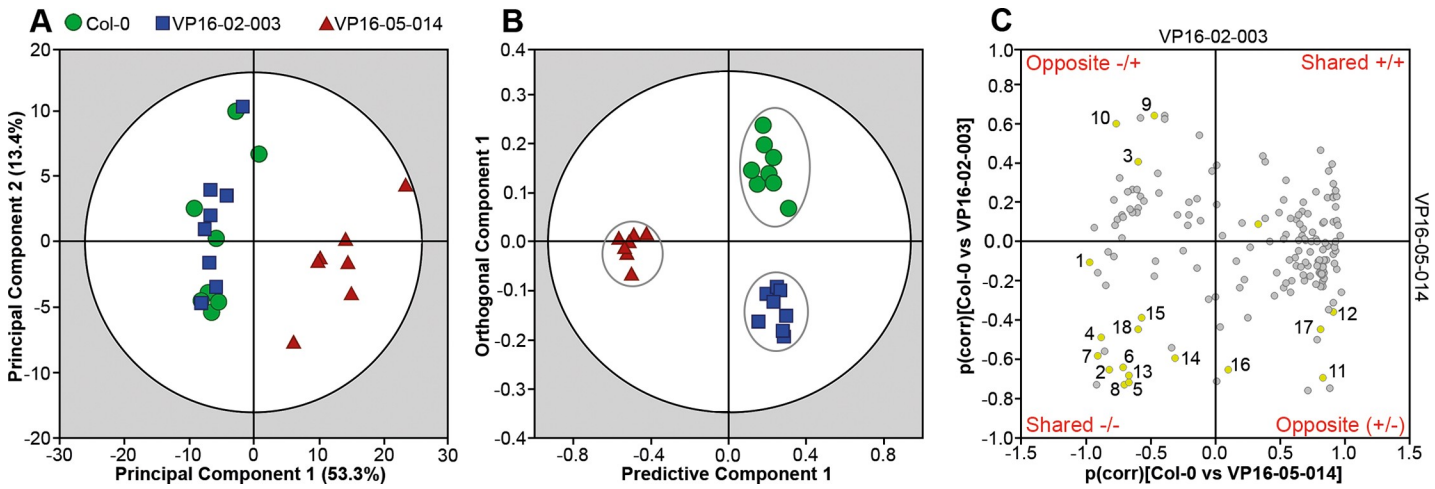

Fig 3. Multivariate analysis of ^{1}H HR-MAS NMR metabolic data collected from *Arabidopsis thaliana* Col-0 (•), VP16-02-003 (■) and VP16-05-014 (▲). (A) PCA score plot with $R^2X = 0.761$ and $Q^2 = 0.611$. The dark circle shows the 95% confidence interval using Hotelling T^2 statistics. (B) OPLS-DA score plot with $R^2X = 0.849$, $R^2Y = 0.942$, $Q^2 = 0.603$, which indicates separation between the Col-0, VP16-02-003 and VP16-05-014 *Arabidopsis* plants based on their metabolic profile. The dark circle represents the Hotelling T^2 interval with 95% confidence. (C) SUS plot represents biomarkers responsible for the separation in the score plot. 1. Fumaric acid; 2. Malic acid; 3. Lactic acid; 4. Fructose; 5. Glucose; 6. Myo-inositol; 7. Choline; 8. Betaine; 9. L-alanine; 10. β-alanine; 11. L-asparagine; 12. L-aspartic acid; 13. L-glutamic acid; 14. L-glutamine; 15. L-glycine; 16. L-lysine; 17. L-phenylalanine; 18. L-tyrosine.

https://doi.org/10.1371/journal.pone.0209695.g003

be of good quality and has an accurate prediction. The score plot also shows that the biological variation for the VP16-02-003 or VP16-05-014 is less than for the wild-type *Arabidopsis* Col-0.

A Shared and Unique Structures (SUS) plot can be a powerful method to identify potential biomarkers for the enhanced growth characteristics for both mutants [26]. To obtain a SUS plot, two separate OPLS-DA models (Col-0 versus VP16-02-003 and Col-0 versus VP16-05-014) were generated from the metabolic profiles (S2 Fig). The correlation coefficients of the

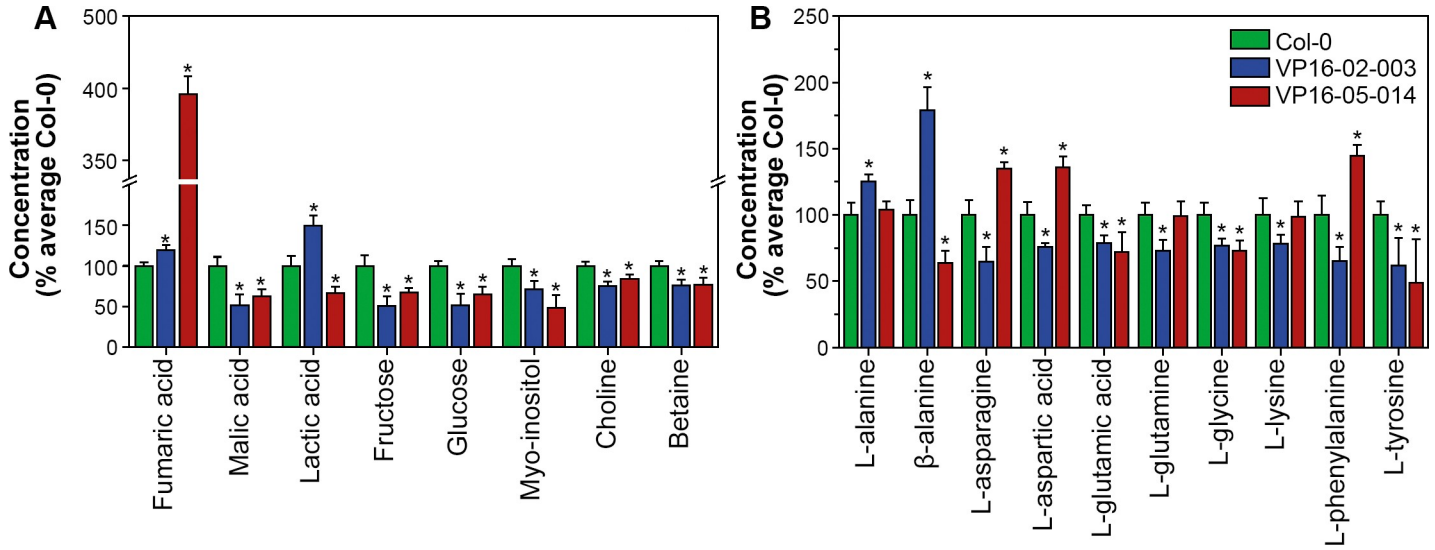

Fig 4. Metabolic alterations in the leaf of *Arabidopsis thaliana* VP16-02-003 and VP16-05-014 plants as compared to Col-0 plants grown in a 12h-light/12h-dark regime by ^{1}H HR-MAS NMR. (A) Relative levels of organic acids, sugars, sugar alcohol, precursor of cell wall components and organic osmolyte in leaves of VP16-02-003 and VP16-05-014 plants in comparison to the level in Col-0. (B) Relative levels of free amino acids in leaves of VP16-02-003 and VP16-05-014 plants in comparison to Col-0. Concentrations are represented by the mean ± SEM averaged over n = 8 samples. The asterisks (*) indicate significant differences between concentrations for Col-0 and mutants, calculated with Student's t-test ($p < 0.05$).

https://doi.org/10.1371/journal.pone.0209695.g004

predictive component p(corr) for both models are plotted against each other in Fig 3C. Concentrations of metabolites plotted in the upper right corner of the SUS-plot increased and those plotted in the lower left corner decreased in both mutants as compared to Col-0. The upper left corner and lower right corner of the SUS-plot contain metabolites with anticorrelated concentrations in the two mutants in comparison to Col-0. Eighteen biomarkers were determined from the SUS plot which show variation between Col-0, VP16-02-003 and VP16-05-014 mutants, including organic acids (fumaric acid, malic acid, lactic acid), sugars (fructose, glucose), a sugar alcohol (myo-inositol), precursor of cell wall components (choline), an organic osmolyte (betaine) and free amino acids (L-alanine, β-alanine, L-asparagine, L-aspartic acid, L-glutamic acid, L-glutamine, L-glycine, L-lysine, L-phenylalanine and L-tyrosine). Most of the identified biomarkers are primary metabolites directly involved in essential processes as growth, development and defence [32,33]. This provides evidence that the larger rosette surface area phenotype of both mutants involves re-allocation of primary resources.

Metabolic evidence for altered growth-defence trade-off in the VP16-02-003 and VP16-05-014 mutants

The quantitative analysis of the metabolites that show significant variation between Col-0, VP16-02-003 and VP16-05-014 plants is shown in Fig 4.

Organic acids, like fumaric acid and malic acid, play an important role in the major carbon metabolism involving glycolysis, the tricarboxylic acid (TCA) cycle, and the photorespiration cycle [34,35]. The fumaric acid level was significantly elevated by 19.5% in the VP16-02-003 mutant and by 295.8% in the VP16-05-014 mutant (Fig 4A). The primary metabolite fumaric acid participates in multiple pathways in plant metabolism and is considered to be one of the major forms of fixed carbon in some C3 plants, including *Arabidopsis* [15,36]. In particular, fumaric acid can accumulate to levels of several milligrams per gram fresh weight in *Arabidopsis* leaves, often exceeding concentrations of starch and soluble sugars [36].

In contrast to fumaric acid, the malic acid level is reduced for both mutants (Fig 4A). Malic acid is involved in various physiological functions in the plant cells, such as supplying NADH for nitrate reduction and carbon skeletons and delivering NADPH for fatty acid biosynthesis [37]. The observed reduced malic acid level for both mutants can be a consequence of its enhanced utilization in downstream pathways involved in the growth promoting phenotype [38]. The role of lactic acid in the leaves of *Arabidopsis thaliana* is not very clear. It has been reported to play a role in plant defence against pathogens [38]. Also, a growth promoting effect of lactic acid has been reported earlier [39,40]. In our study, no common trend was observed in the levels of lactic acid in two mutants. The lactic acid concentration was elevated by 49.1% in the VP16-02-003 mutant ($p < 0.05$), and reduced by 33.2% in the VP16-05-014 mutant ($p < 0.05$) (Fig 4A). Thus no growth promoting effect of lactic acid can be generalized from our study.

Primary sugars in plants such as glucose, fructose, and sucrose, are produced during photosynthesis, provide the primary energy supply and serve as storage metabolites in plants. These sugars have a regulatory role in photosynthesis, growth and development and as a signalling molecule to modulate gene expression [41]. The levels of fructose and glucose were in both the VP16-02-003 and the VP16-05-014 mutants significantly decreased in comparison to Col-0 (Fig 4A). Decrease in glucose level is also in line with downregulation of glucan 1,3-beta-glucosidase (AT1G64760) seen in transcriptome data of these two mutant (S1 Table) [12]. Glucan endo-1,3-beta-glucosidase is involved in carbohydrate metabolism and has been shown to be linked with plant defence to fungus and nematodes [42]. Although the stress response is a very dynamic process and differs for every stress type, soluble sugar concentrations are altered

during defence and strongly decrease in response to different forms of abiotic stress, as energy is needed to operate defence mechanisms. In general low sugar concentrations lead to an impaired abiotic and biotic stress response [41,43].

Myo-inositol is a signalling metabolite in *Arabidopsis thaliana* [44]. It is involved in stress response, regulation of cell death and cell wall biosynthesis [45,46]. The concentration of myo-inositol was reduced by 28.3% ($p < 0.05$) in the VP16-02-003 mutant and by 51.7% in the VP16-05-014 mutant ($p < 0.05$) (Fig 4A). A reduced pool of myo-inositol in the VP16-02-003 and VP16-05-014 mutant may reflect an impaired defence pathway regulation in these mutants. For instance, in a previous study, the reduced level of myo-inositol was observed in the *mips1* mutant, a mutant which shows increased sensitivity to reactive oxygen species stress [45].

Choline is an important precursor for membrane phospholipids in plants. Choline can be oxidized in a 2-step reaction via betaine aldehyde to betaine (glycine betaine, *N*,*N*,*N*-trimethyl-glycine). Accumulation of betaine in *Arabidopsis thaliana* leads to a higher tolerance for abiotic stress [47,48]. The choline and betaine levels in the VP16-02-003 and the VP16-05-014 mutant were both significantly reduced in comparison to the wild-type Col-0 (Fig 4A). This is in line with less available resources for stress resistance and defence and low concentrations of the soluble primary carriers malic acid, fructose and glucose, as well as more storage in the form of fumaric acid.

Amino acids are essential precursors for a wide range of cellular components like proteins, nucleotides, chlorophylls and nitrogen-containing compounds [49,50]. Fig 4B shows the concentrations of free amino acids in the VP16-02-003 and the VP16-05-014 mutant in comparison to *Arabidopsis* Col-0. In both VP16-02-003 and VP16-05-014 mutants, levels of L-glutamic acid, L-glycine and L-tyrosine were decreased relative to Col-0. This decline is consistent with overall decrease in total free amino acids shown in Table 1. The pattern of decline in these amino acids may be associated with decrease in the level of sugars. From earlier studies, it is known that a decreased level of sugar leads to the inhibition of amino acid biosynthesis [49]. Since, amino acid metabolism plays a regulatory role in the response to stress [50][51], a decline in the levels of these free amino acids for both mutants may reflects their reduced investments to defence responses against stress. A decline in glycine in both mutants may be linked with downregulation of Glycine-rich RNA binding proteins observed in transcriptome data of these mutants. Glycine-rich proteins are known to be involved in plant stress responses [52]. Downregulation of Glycine-rich RNA binding proteins together with low glycine levels thus signify low defence response of VP16-02-003 and VP16-05-014 mutant. The levels of other free amino acids such as L-asparagine, L-aspartic acid, L-glutamine, L-lysine and L-phenylalanine were also lower in VP16-02-003 mutant in contrast to Col-0. However, their levels either did not change or increased in VP16-02-003 mutant with respect to Col-0. The reason for the differences in some of the amino acid pattern in two mutants is presently not understood. Interestingly the levels of L-alanine and β-alanine were significantly higher in the VP16-02-003 mutant in comparison to the wild-type Col-0. An increase in alanine under sulphur limitation has been reported earlier [53]. Transcriptome analysis of this mutant has revealed downregulation of sulphate metabolism genes [12]. High levels of alanine in the VP16-02-003 mutant may thus be connected to reduced sulphur fixation.

The changes of metabolic profiles for the VP16-02-003 and the VP16-05-014 mutant that share a larger rosette surface area phenotype are mostly associated with the response to stress. These results are in line with our earlier transcriptome analysis, which shows that many genes that are downregulated in both mutants are involved in defence processes [12]. Recently, Fusari et al. [54] have investigated the genetic architecture of central metabolism by mapping metabolite quantitative trait loci (QTL). The results of genome-wide associated mapping

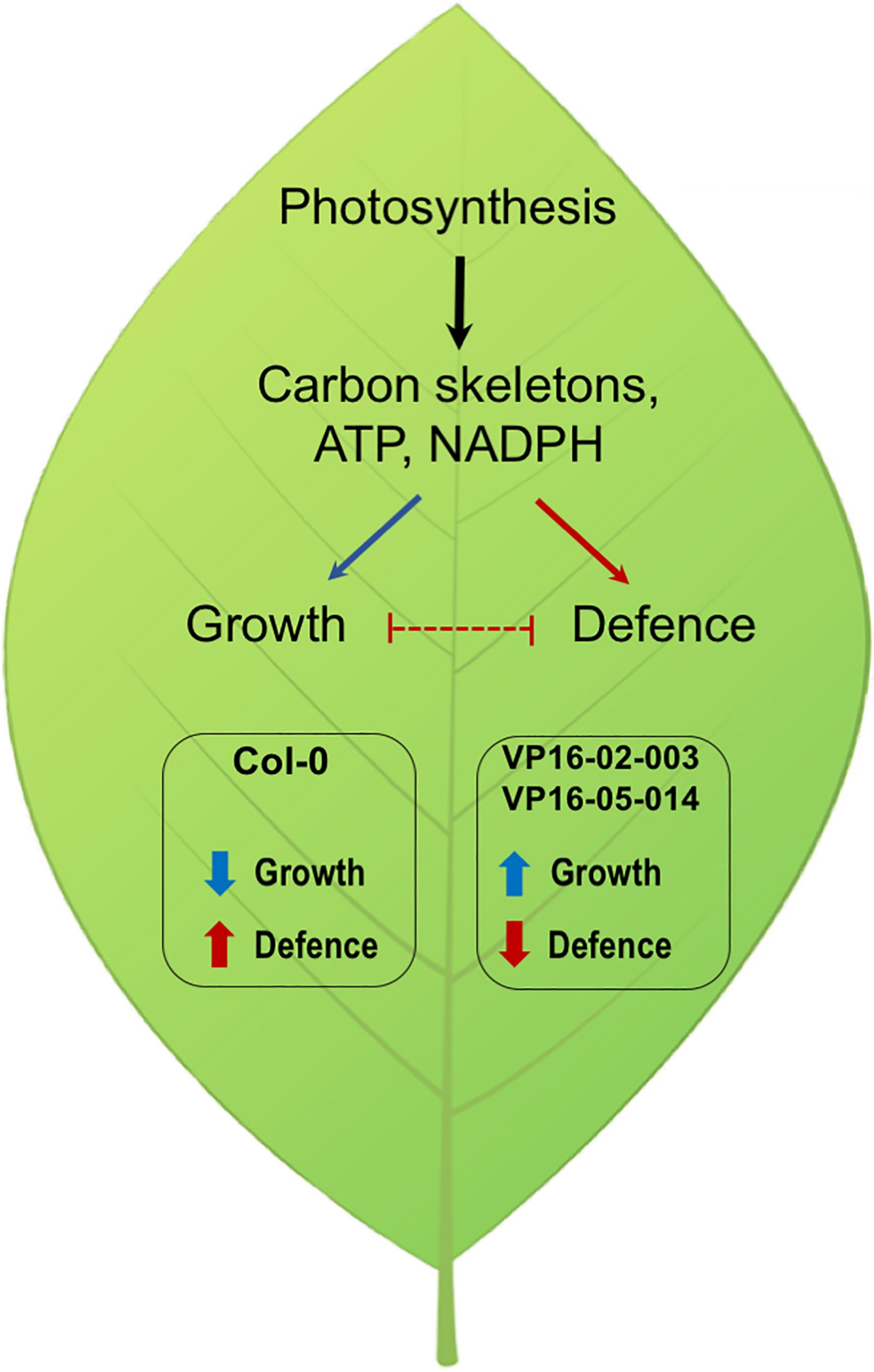
Photosynthesis
Carbon skeletons,
ATP, NADPH
Growth
Defence
Col-0
Growth
Defence
VP16-02-003
VP16-05-014
Growth
Defence

Fig 5. Proposed model for the different growth-defence trade-off in the VP16-02-003 and VP16-05-014 mutant with a larger rosette surface area shared phenotype in comparison to wild-type *Arabidopsis thaliana* Col-0.

https://doi.org/10.1371/journal.pone.0209695.g005

clearly revealed a well-defined trade-off between growth and defence in *Arabidopsis* which involve a fine-tuning of central metabolism. Thus, adaptation of the physiological function in *Arabidopsis thaliana* requires balancing of primary metabolites [55]. The trade-off between plant growth and defence implies that both are negatively correlated [55–57]. Hence the growth will improve when the defence system is less active in plants. Our results show that the VP16-02-003 and the VP16-05-014 mutants have a reduced defence response against stress (Fig 5), which shifts the balance toward enhanced growth which involves changes in metabolism. Some of the recent leaf and apical damage studies, show mixed results on whether a trade-off exist between growth, tolerance and defence [57–61]. Thus, future studies on damaged and undamaged states of VP16-02-003 and VP16-05-014 mutants will be important to dissect out the mechanistic insight into growth-defence conflict.

The fundamental understanding about linking the gene regulatory network to the physiological response obtained in this work paves the way for further investigations. In particular, it is known that physiological functions in *Arabidopsis* are regulated by the circadian cycle [62,63] and analysis of rhythmic patterns of the biomarkers in the VP16-02-003 and the VP16-05-014 mutants may help to resolve the underlying mechanisms involved in growth-defence trade-off.

Conclusion

In this study, the metabolic profiles of the *Arabidopsis thaliana* mutant lines VP16-02-003 and VP16-05-014 with a larger rosette surface were further phenotyped and also investigated with the HR-MAS NMR-based metabolomics approach. The results provide converging evidence that the alteration of the metabolic profile of both mutants is due to lower defence responses against stress. Growth-defence trade-offs will thus have to be acknowledged for when trying to generate crops with improved growth characteristics.

Supporting information

S1 Fig. Principal component analysis (PCA) score plots derived from one-dimensional ^{1}H HR-MAS NMR spectra of *Arabidopsis thaliana* Col-0 (•), VP16-02-003 (■) and VP16-05-014 (▲) with the outlier for VP16-05-014. A three components model with $R^2X = 0.756$, $Q^2 = 0.585$. The dark ellipse represents the Hotelling T^2 interval with 95% confidence.
(TIF)

S2 Fig. Score plot of the orthogonal partial least square-discriminant (OPLS-DA) model derived from ^{1}H HR-MAS spectra of *Arabidopsis thaliana* Col-0 and VP16-02-003 (A) and Col-0 and VP16-05-014 (B). For model A: R2X = 0.865, R2Y = 0.999, Q2 = 0.568. For model B: R2X = 0.666, R2Y = 0.975, Q2 = 0.933. The dark ellipse shows the 95% confidence interval using Hotelling T2 statistics.
(TIF)

S1 Table. Downregulated genes in the VP16-02-003 and VP16-05-014 mutant and the related GO terms referred to stress or defence.
(DOCX)

S2 Table. Measured metabolites in leaves of Col-0, VP16-02-003 and VP16-05-014 plants and their chemical shift assignment in 1H HR-MAS NMR spectrum.
(DOCX)

Acknowledgments

The authors thank Fons Lefeber and Karthick Babu Sai Sankar Gupta for their assistance during various stages of the HR-MAS NMR measurements.

Author Contributions

Conceptualization: Dieuwertje Augustijn, Niels van Tol, Bert J. van der Zaal, Huub J. M. de Groot, A. Alia.

Data curation: Dieuwertje Augustijn, Niels van Tol.

Formal analysis: Dieuwertje Augustijn, Niels van Tol.

Funding acquisition: Bert J. van der Zaal, Huub J. M. de Groot, A. Alia.

Investigation: Dieuwertje Augustijn, Niels van Tol, Bert J. van der Zaal.

Methodology: Dieuwertje Augustijn, Niels van Tol, Bert J. van der Zaal, Huub J. M. de Groot, A. Alia.

Project administration: Bert J. van der Zaal, Huub J. M. de Groot, A. Alia.

Software: Dieuwertje Augustijn.

Supervision: Bert J. van der Zaal, Huub J. M. de Groot, A. Alia.

Validation: Dieuwertje Augustijn, Niels van Tol, Huub J. M. de Groot.

Visualization: A. Alia.

Writing – original draft: Dieuwertje Augustijn, A. Alia.

Writing – review & editing: Dieuwertje Augustijn, Niels van Tol, Bert J. van der Zaal, Huub J. M. de Groot, A. Alia.

References

1. Edgerton MD. Increasing Crop Productivity to Meet Global Needs for Feed, Food, and Fuel. Plant Physiology. American Society of Plant Biologists; 2009; 149: 7–13. https://doi.org/10.1104/pp.108.130195 PMID: 19126690
2. Haberl H, Beringer T, Bhattacharya SC, Erb K-H, Hoogwijk M. The global technical potential of bio-energy in 2050 considering sustainability constraints. Current Opinion in Environmental Sustainability. Elsevier Science; 2010; 2: 394–403. https://doi.org/10.1016/j.cosust.2010.10.007 PMID: 24069093
3. Tilman D, Cassman KG, Matson PA, Naylor R, Polasky S. Agricultural sustainability and intensive production practices. Nature. 2002; 418: 671–677. https://doi.org/10.1038/nature01014 PMID: 12167873
4. Davis KF, Gephart JA, Emery KA, Leach AM, Galloway JN, D'Odorico P. Meeting future food demand with current agricultural resources. Global Environmental Change. 2016; 39: 125–132.
5. Mba C, Guimaraes EP, Ghosh K. Re-orienting crop improvement for the changing climatic conditions of the 21st century. Agriculture & Food Security. BioMed Central; 2012; 1: 7–17.
6. Kumar A, Pathak RK, Gupta SM, Gaur VS, Pandey D. Systems Biology for Smart Crops and Agricultural Innovation: Filling the Gaps between Genotype and Phenotype for Complex Traits Linked with Robust Agricultural Productivity and Sustainability. OMICS. 2015; 19: 581–601. https://doi.org/10.1089/omi.2015.0106 PMID: 26484978
7. Rommens CM, Haring MA, Swords K, Davies HV, Belknap WR. The intragenic approach as a new extension to traditional plant breeding. Trends in Plant Science. 2007; 12: 397–403. https://doi.org/10.1016/j.tplants.2007.08.001 PMID: 17692557

8. Andolfo G, Iovieno P, Frusciante L, Ercolano MR. Genome-Editing Technologies for Enhancing Plant Disease Resistance. Front Plant Sci. 2016; 7: 19035. https://doi.org/10.3389/fpls.2016.01813 PMID: 27990151
9. van Tol N, van der Zaal BJ. Artificial transcription factor-mediated regulation of gene expression. Plant Science. Elsevier Ireland Ltd; 2014; 225: 58–67. https://doi.org/10.1016/j.plantsci.2014.05.015 PMID: 25017160
10. Li J, Blue R, Zeitler B, Strange TL, Pearl JR, Huizinga DH, et al. Activation domains for controlling plant gene expression using designed transcription factors. Plant Biotechnology Journal. 2013; 11: 671–680. https://doi.org/10.1111/pbi.12057 PMID: 23521778
11. Lindhout BI, Pinas JE, Hooykaas PJJ, van der Zaal BJ. Employing libraries of zinc finger artificial transcription factors to screen for homologous recombination mutants in Arabidopsis. The Plant Journal. Blackwell Publishing Ltd; 2006; 48: 475–483. https://doi.org/10.1111/j.1365-313X.2006.02877.x PMID: 17052325
12. Tol NV, Rolloos M, Pinas JE, Henkel CV, Augustijn D, Hooykaas PJJ, et al. Enhancement of Arabidopsis growth characteristics using genome interrogation with artificial transcription factors. PLoS One. Public Library of Science; 2017; 12: e0174236. https://doi.org/10.1371/journal.pone.0174236 PMID: 28358915
13. Sheth BP, Thaker VS. Plant systems biology: insights, advances and challenges. Planta. 2014; 240: 33–54. https://doi.org/10.1007/s00425-014-2059-5 PMID: 24671625
14. Meyer RC, Steinfath M, Lisec J, Becher M, Witucka-Wall H, Törjék O, et al. The metabolic signature related to high plant growth rate in Arabidopsis thaliana. PNAS. National Acad Sciences; 2007; 104: 4759–4764. https://doi.org/10.1073/pnas.0609709104 PMID: 17360597
15. Augustijn D, Roy U, van Schadewijk R, de Groot HJM, Alia A. Metabolic Profiling of Intact Arabidopsis thaliana Leaves during Circadian Cycle Using 1H High Resolution Magic Angle Spinning NMR. PLoS One. 2016; 11: e0163258. https://doi.org/10.1371/journal.pone.0163258 PMID: 27662620
16. DuBois M, Gilles KA, Hamilton JK, Rebers PA, Smith F. Colorimetric Method for Determination of Sugars and Related Substances. Anal Chem. American Chemical Society; 1956; 28: 350–356. https://doi.org/10.1021/ac60111a017
17. Gepstein S, Thimann KV. The role of ethylene in the senescence of oat leaves. Plant Physiology. 1981; 68: 349–354. PMID: 16661915
18. Gibon Y, Blaesing OE, Hannemann J, Carillo P, Höhne M, Hendriks JHM, et al. A Robot-based platform to measure multiple enzyme activities in Arabidopsis using a set of cycling assays: comparison of changes of enzyme activities and transcript levels during diurnal cycles and in prolonged darkness. Plant Cell. American Society of Plant Biologists; 2004; 16: 3304–3325. https://doi.org/10.1105/tpc.104.025973 PMID: 15548738
19. Bradford MM. A rapid and sensitive method for the quantitation of microgram quantities of protein utilizing the principle of protein-dye binding. Analytical Biochemistry. 1976; 72: 248–254. https://doi.org/10.1016/0003-2697(76)90527-3 PMID: 942051
20. Smith AM, Zeeman SC. Quantification of starch in plant tissues. Nat Protocols. Nature Publishing Group; 2006; 1: 1342–1345. https://doi.org/10.1038/nprot.2006.232 PMID: 17406420
21. Meiboom S, Gill D. Modified Spin-Echo Method for Measuring Nuclear Relaxation Times. Review of Scientific Instruments. 1958; 29: 688–691. https://doi.org/10.1063/1.1716296
22. Euceda LR, Giskeodegard GF, Bathen TF. Preprocessing of NMR metabolomics data. Scand J Clin Lab Invest. 2015; 75: 193–203. https://doi.org/10.3109/00365513.2014.1003593 PMID: 25738209
23. Worley B, Powers R. Multivariate Analysis in Metabolomics. CMB. 2012; 1: 92–107. https://doi.org/10.2174/2213235X11301010092 PMID: 26078916
24. Westerhuis JA, Hoefsloot HCJ, Smit S, Vis DJ, Smilde AK, van Velzen EJJ, et al. Assessment of PLSDA cross validation. Metabolomics. 2008; 4: 81–89.
25. Trygg J, Holmes E, Lundstedt T. Chemometrics in metabonomics. J Proteome Res. 2007; 6: 469–479. https://doi.org/10.1021/pr060594q PMID: 17269704
26. Wiklund S, Johansson E, Sjöström L, Mellerowicz EJ, Edlund U, Shockcor JP, et al. Visualization of GC/TOF-MS-Based Metabolomics Data for Identification of Biochemically Interesting Compounds Using OPLS Class Models. Anal Chem. American Chemical Society; 2008; 80: 115–122. https://doi.org/10.1021/ac0713510 PMID: 18027910
27. Akiyama K, Chikayama E, Yuasa H, Shimada Y, Tohge T, Shinozaki K, et al. PRIMe: a Web site that assembles tools for metabolomics and transcriptomics. In Silico Biol. 2008; 8: 339–345. PMID: 19032166
28. Sakurai T, Yamada Y, Sawada Y, Matsuda F, Akiyama K, Shinozaki K, et al. PRIMe Update: innovative content for plant metabolomics and integration of gene expression and metabolite accumulation. Plant

Cell Physiol. Oxford University Press; 2013; 54: e5–e5. https://doi.org/10.1093/pcp/pcs184 PMID: 23292601

29. Sulpice R, Pyl E-T, Ishihara H, Trenkamp S, Steinfath M, Witucka-Wall H, et al. Starch as a major integrator in the regulation of plant growth. PNAS. 2009; 106: 10348–10353. https://doi.org/10.1073/pnas.0903478106 PMID: 19506259

30. Govindaraju V, Young K, Maudsley AA. Proton NMR chemical shifts and coupling constants for brain metabolites. NMR Biomed. 2000; 13: 129–153. PMID: 10861994

31. Ulrich EL, Akutsu H, Doreleijers JF, Harano Y, Ioannidis YE, Lin J, et al. BioMagResBank. Nucleic Acids Res. 2008; 36: D402–8. https://doi.org/10.1093/nar/gkm957 PMID: 17984079

32. Schwachtje J, Fischer A, Erban A, Kopka J. Primed primary metabolism in systemic leaves: a functional systems analysis. Sci Rep. 2018; 8: 216. https://doi.org/10.1038/s41598-017-18397-5 PMID: 29317679

33. Rojas CM, Senthil-Kumar M, Tzin V, Mysore KS. Regulation of primary plant metabolism during plant-pathogen interactions and its contribution to plant defense. Front Plant Sci. Frontiers Media S.A; 2014; 5: 17. https://doi.org/10.3389/fpls.2014.00017 PMID: 24575102

34. Zell MB, Fahnenstich H, Maier A, Saigo M, Voznesenskaya EV, Edwards GE, et al. Analysis of Arabidopsis with highly reduced levels of malate and fumarate sheds light on the role of these organic acids as storage carbon molecules. Plant Physiology. American Society of Plant Biologists; 2010; 152: 1251–1262. https://doi.org/10.1104/pp.109.151795 PMID: 20107023

35. Igamberdiev AU, Eprintsev AT. Organic Acids: The Pools of Fixed Carbon Involved in Redox Regulation and Energy Balance in Higher Plants. Front Plant Sci. 2016; 7: 513. https://doi.org/10.3389/fpls.2016.00513

36. Chia DW, Yoder TJ, Reiter W-D, Gibson SI. Fumaric acid: an overlooked form of fixed carbon in Arabidopsis and other plant species. Planta. Springer-Verlag; 2000; 211: 743–751. https://doi.org/10.1007/s004250000345 PMID: 11089689

37. Fahnenstich H, Saigo M, Niessen M, Zanor MI, Andreo CS, Fernie AR, et al. Alteration of Organic Acid Metabolism in Arabidopsis Overexpressing the Maize C4 NADP-Malic Enzyme Causes Accelerated Senescence during Extended Darkness. Plant Physiology. American Society of Plant Biologists; 2007; 145: 640–652. https://doi.org/10.1104/pp.107.104455 PMID: 17885087

38. Maurino VG, Engqvist MKM. 2-Hydroxy Acids in Plant Metabolism. Arabidopsis Book. American Society of Plant Biologists; 2015; 13: e0182. https://doi.org/10.1199/tab.0182 PMID: 26380567

39. Kinnersley AM, Scott TC, Yopp JH, Whitten GH. Promotion of plant growth by polymers of lactic acid. Plant Growth Regulation. 1990; 9: 137–146.

40. Yoshikawa M, Hirai N, Wakabayashi K, Sugizaki H, Iwamura H. Succinic and lactic acids as plant growth promoting compounds produced by rhizospheric Pseudomonas putida. Can J Microbiol. NRC Research Press; 1993; 39: 1150–1154. https://doi.org/10.1139/m93-173

41. Rosa M, Prado C, Podazza G, Interdonato R, Gonzalez JA, Hilal M, et al. Soluble sugars—metabolism, sensing and abiotic stress: a complex network in the life of plants. Plant Signal Behav. 2009; 4: 388–393. https://doi.org/10.4161/psb.4.5.8294 PMID: 19816104

42. Hamamouch N, Li C, Hewezi T, Baum TJ, Mitchum MG, Hussey RS, et al. The interaction of the novel 30C02 cyst nematode effector protein with a plant β-1,3-endoglucanase may suppress host defence to promote parasitism. Journal of Experimental Botany. Oxford University Press; 2012; 63: 3683–3695. https://doi.org/10.1093/jxb/ers058 PMID: 22442414

43. Morkunas I, Ratajczak L. The role of sugar signaling in plant defense responses against fungal pathogens. Acta Physiol Plant. 2014; 36: 1607–1619.

44. Loewus FA, Murthy PPN. myo-Inositol metabolism in plants. Plant Science. 2000; 150: 1–19.

45. Donahue JL, Alford SR, Torabinejad J, Kerwin RE, Nourbakhsh A, Ray WK, et al. The Arabidopsis thaliana Myo-Inositol 1-Phosphate Synthase1 Gene Is Required for Myo-inositol Synthesis and Suppression of Cell Death. Plant Cell. American Society of Plant Biologists; 2010; 22: 888–903. https://doi.org/10.1105/tpc.109.071779 PMID: 20215587

46. Meng PH, Raynaud C, Tcherkez G, Blanchet S, Massoud K, Domenichini S, et al. Crosstalks between Myo-Inositol Metabolism, Programmed Cell Death and Basal Immunity in Arabidopsis. Bendahmane M, editor. PLoS One. Public Library of Science; 2009; 4: e7364. https://doi.org/10.1371/journal.pone.0007364 PMID: 19812700

47. Sakamoto A, Murata N. The role of glycine betaine in the protection of plants from stress: clues from transgenic plants. Plant Cell Environ. Blackwell Science Ltd; 2002; 25: 163–171. https://doi.org/10.1046/j.0016-8025.2001.00790.x PMID: 11841661

48. Huang J, Rozwadowski K, Bhinu VS, Schafer U, Hannoufa A. Manipulation of sinapine, choline and betaine accumulation in Arabidopsis seed: towards improving the nutritional value of the meal and

enhancing the seedling performance under environmental stresses in oilseed crops. Plant Physiol Biochem. 2008; 46: 647–654. https://doi.org/10.1016/j.plaphy.2008.04.014 PMID: 18515127

49. Stitt M, Muller C, Matt P, Gibon Y, Carillo P, Morcuende R, et al. Steps towards an integrated view of nitrogen metabolism. Journal of Experimental Botany. 2002; 53: 959–970. PMID: 11912238

50. Hildebrandt TM, Nunes Nesi A, Araujo WL, Braun H-P. Amino Acid Catabolism in Plants. Molecular Plant. 2015; 8: 1563–1579. https://doi.org/10.1016/j.molp.2015.09.005 PMID: 26384576

51. Pratelli R, Pilot G. Regulation of amino acid metabolic enzymes and transporters in plants. Journal of Experimental Botany. 2014; 65: 5535–5556. https://doi.org/10.1093/jxb/eru320 PMID: 25114014

52. Czolpinska M, Rurek M. Plant Glycine-Rich Proteins in Stress Response: An Emerging, Still Prospective Story. Front Plant Sci. 2018; 9: 302. https://doi.org/10.3389/fpls.2018.00302 PMID: 29568308

53. Giordano M, Pezzoni V, Hell R. Strategies for the Allocation of Resources under Sulfur Limitation in the Green Alga Dunaliella salina. Plant Physiology. American Society of Plant Physiologists; 2000; 124: 857–864. PMID: 11027733

54. Fusari CM, Kooke R, Lauxmann MA, Annunziata MG, Enke B, Hoehne M, et al. Genome-Wide Association Mapping Reveals That Specific and Pleiotropic Regulatory Mechanisms Fine-Tune Central Metabolism and Growth in Arabidopsis. Plant Cell. 2017; 29: 2349–2373. https://doi.org/10.1105/tpc.17.00232 PMID: 28954812

55. Caretto S, Linsalata V, Colella G, Mita G, Lattanzio V. Carbon Fluxes between Primary Metabolism and Phenolic Pathway in Plant Tissues under Stress. Int J Mol Sci. MDPI; 2015; 16: 26378–26394. https://doi.org/10.3390/ijms161125967 PMID: 26556338

56. Huot B, Yao J, Montgomery BL, He SY. Growth–Defense Tradeoffs in Plants: A Balancing Act to Optimize Fitness. Molecular Plant. 2014; 7: 1267–1287. https://doi.org/10.1093/mp/ssu049 PMID: 24777989

57. Zust T, Agrawal AA. Trade-Offs Between Plant Growth and Defense Against Insect Herbivory: An Emerging Mechanistic Synthesis. Annu Rev Plant Biol. 2017; 68: 513–534. https://doi.org/10.1146/annurev-arplant-042916-040856 PMID: 28142282

58. Guo T, Chen K, Dong N-Q, Shi C-L, Ye W-W, Gao J-P, et al. GRAIN SIZE AND NUMBER1Negatively Regulates the OsMKKK10-OsMKK4-OsMPK6 Cascade to Coordinate the Trade-off between Grain Number per Panicle and Grain Size in Rice. Plant Cell. 2018; 30: 871–888. https://doi.org/10.1105/tpc.17.00959 PMID: 29588389

59. Gloss AD, Brachi B, Feldmann MJ, Groen SC, Bartoli C, Gouzy J, et al. Genetic variants affecting plant size and chemical defenses jointly shape herbivory in Arabidopsis. 2017. https://doi.org/10.1101/156299

60. Scholes DR, Paige KN. Plasticity in ploidy: a generalized response to stress. Trends in Plant Science. 2015; 20: 165–175. https://doi.org/10.1016/j.tplants.2014.11.007 PMID: 25534217

61. Mesa JM, Scholes DR, Juvik JA, Paige KN. Molecular constraints on resistance-tolerance trade-offs. Ecology. Wiley-Blackwell; 2017; 98: 2528–2537. https://doi.org/10.1002/ecy.1948 PMID: 28715081

62. Bendix C, Marshall CM, Harmon FG. Circadian Clock Genes Universally Control Key Agricultural Traits. Molecular Plant. 2015; 8: 1135–1152. https://doi.org/10.1016/j.molp.2015.03.003 PMID: 25772379

63. Greenham K, McClung CR. Integrating circadian dynamics with physiological processes in plants. Nat Rev Genet. Nature Publishing Group; 2015; 16: 598–610. https://doi.org/10.1038/nrg3976 PMID: 26370901